Modeling Potential Shallow Landslides over Large Areas with SliDisp$^+$

Daniel Tobler, Rachel Riner, and Robert Pfeifer

Abstract

The deterministic model SliDisp$^+$ calculates the potential detachment zones of shallow landslides. It is a grid-based model using an infinite slope analysis to calculate the safety factors F (ratio of retaining and driving forces) for each cell.

The input data consists of the slope topography, soil strength parameters, depths and shapes of potential shear planes, and the hydraulic behavior. The variables are derived from a digital elevation model (DEM), geological, geotechnical, and pedological documents, or field investigations. From this data the soil is classified over large areas. For each cell, the critical slope angle as well as the soil cohesion is determined.

Studies in several test areas showed that pedological aspects as well as joint water-input from underlying rock must be taken into account. Combined with the run-out model SliDepot, SliDisp$^+$ calculates the extent of potential landslides over large areas and thus can be applied for spatial planning and optimized positioning of protection measures.

Keywords

Shallow landslide modeling • SliDisp$^+$ • SliDepot

Introduction

In mountain regions many residential areas as well as important lifelines are generally exposed to potential shallow landslide events (Griffiths et al. 2002). Spatial planning is one of the major key elements in protection against natural hazards and requires a comprehensive assessment of landslide processes (Glade et al. 2005; Sidle and Ochiai 2006). By applying process models, the extent of potential landslides can be calculated over large areas (Guzzetti et al. 2006; Zolfaghari and Heath 2008; Dai and Lee 2002). The resulting maps provide a quick identification of endangered areas with conflicts between hazards and land use. It is the base on which to set priorities for a more accurate hazard assessment.

Since 2000, the authors have applied the process model SliDisp to indicate hazard zones within large administrative areas. Within the same period, the model and the assessment method to gather input-data have been redesigned and improved.

Model SliDisp/SliDisp$^+$

The original model SliDisp was developed by Liener (2000) at the University of Berne. Studies in several test areas showed that the assessment of detachment zones for potential shallow landslides must inevitably take pedological aspects as well as joint water-input from the underlying bedrock into account (Guimarães et al. 2003; Rickli and Bucher 2003; Dahal 2008; Paulin and Bursik 2009). During the last 5 years various modifications were made and the program advanced to SliDisp$^+$ (Riner 2009).

D. Tobler (✉)
Institute of Geography, University of Berne, Hallerstrasse 12, Berne CH-3012, Switzerland

GEOTEST AG, Birkenstrasse 15, Zollikofen CH-3052, Switzerland
e-mail: daniel.tobler@geotest.ch; info@geotest.ch

R. Riner • R. Pfeifer
GEOTEST AG, Birkenstrasse 15, Zollikofen CH-3052, Switzerland
e-mail: info@geotest.ch; info@geotest.ch

C. Margottini et al. (eds.), *Landslide Science and Practice*, Vol. 3,
DOI 10.1007/978-3-642-31310-3_6,

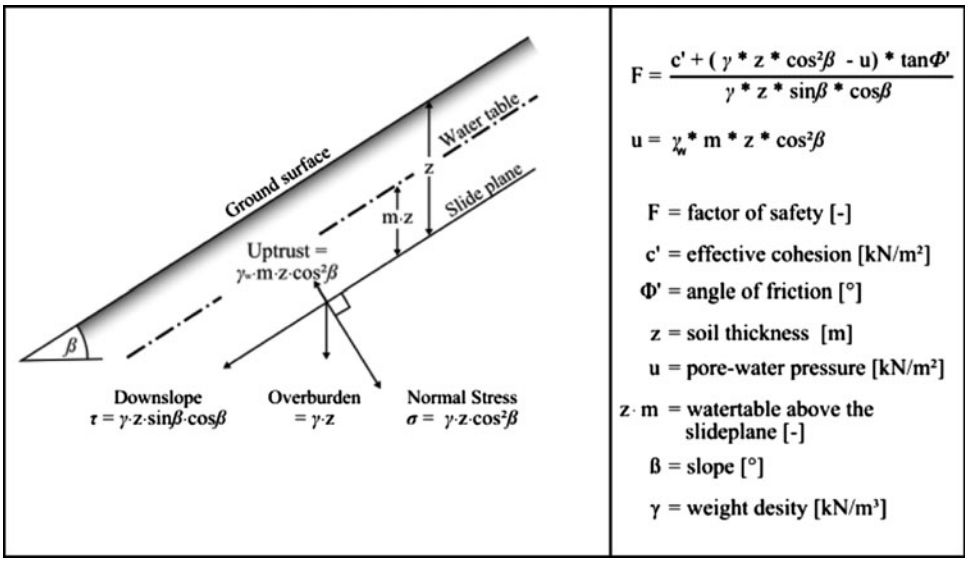

Fig. 1 Principle for the calculation of the factor of safety F for every raster cell (Selby 1993). Indication of all parameters needed for the calculation, except the root cohesion (WK, see Formula 1)

Stability Calculation in SliDisp

SliDisp is a deterministic model which calculates the landslide susceptibility of slopes. The calculation of stability is based on the formula of Selby (1993), whereas the characteristic soil-physics, the thickness of subsoil, the ground water level, the slope, and the force of roots are taken as determining parameters (Fig. 1, Formula 1).

For the model calculation a term for root cohesion (WK) has been added to the original formula of the factor of safety F (Formula 1). This empirical adjusted parameter takes the roots-retaining forces of the vegetation layer into account (Schmidt et al. 2001; Chok et al. 2004; Hales et al. 2009).

$$F = \frac{WK + c' + (\gamma \cdot z \cdot cos^2\beta - \gamma_w \cdot m \cdot z \cdot cos^2\beta) \cdot tan\varphi'}{\gamma \cdot z \cdot sin\beta \cdot cos\beta} \quad (1)$$

The safety factor F is calculated for each cell of the grid, based on the data from the digital elevation model (DEM). If $F < 1$, the cell is potentially instable, and the material can be set into motion by triggering factors. The total of all instable grid elements equals the maximum detachment area (= landslide susceptibility).

The normal variation of shearing parameters is acknowledged by a Monte-Carlo simulation (Kalos and Whitlock 1986). By applying this method, 100 random values are chosen from the deviation of the shearing parameters to calculate the factor of safety (F). With this random combination of parameters, the factor of safety is calculated 100 times for each cell. We assume that both the cohesion and the friction angle show a normal distribution and do not correlate with each other (Lacasse and Nadim 1996).

Areas with more than 60 % of the parameter combination showing a safety factor $F < 1$ are indicated as potential sources. If more than 90 % of the F-values are <1, a medium to large chance of a potential landslide is expected. The data preparation as well as its visualization is carried out by means of a geographic information system (GIS). The calculation of the stability factors is implemented by a C-application and then integrated into the GIS.

Model-Parameter SliDisp

Deterministic models based on the infinite slope analysis (cf. Formula 1) call for strongly simplified model parameters (Dahal 2008). Concretely these are: soil thickness, slope angle, ground water level, shear strength, cohesion, and root strength. The parameters are derived from the variable morphology, the geology, and the geotechnical characteristics of the loose rock and vegetation cover (Guzzetti et al. 2006; cf. Fig. 1). The different parameters and their determination are described in the following sections.

Therefore the three main data sources are the digital elevation model (DEM), geological and geotechnical information (maps, laboratory data, results from field investigations) and pedological datasets (type of soil). Figure 2 demonstrates the relationship or derivation of the different datasets used in SliDisp/SliDisp$^+$.

Morphological Variables

Digital elevation models (DEM) are of central significance as database to assess morphological variables. They serve as basic information to calculate the slope angle and the topographically induced water saturation potential of each grid cell (topographic-index, Beven et al. 1995; Liener et al. 1996). The topographic index corresponds to the natural logarithm of the ratio of drained area of the cell to slope angle β of the cell (cf. Formula 2, Fig. 3). The hydrologically

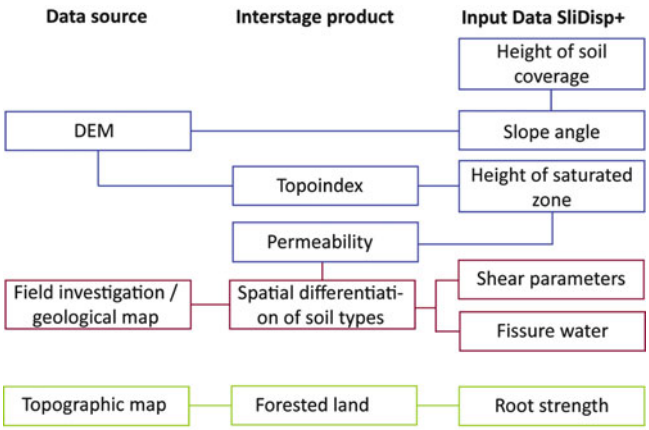

Fig. 2 Derivation of the model-parameters (input data) for the infinite slope model SliDisp/SliDisp+ (Riner 2009)

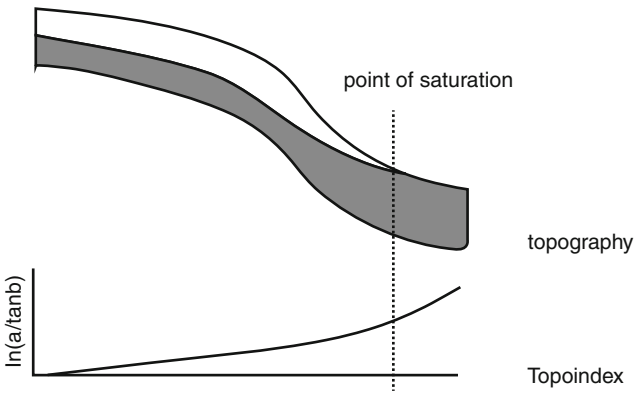

Fig. 3 Relationship between the topography and the topographic index (After Quinn et al. 1995, slightly modified)

relevant morphologies (ridge, flank, basin/dell, channels) are derived from the topo-index values. In a further step, these values serve as a basis to calculate ground water levels.

$$\text{topographic-index} = \ln(a/\tan\beta) \quad (2)$$

Soil Thickness

There are different ways to gain data about the thickness of the soil coverage: from existing datasets (boreholes, soundings, field mapping), from field investigations, and from model calculations (Godt et al. 2008). Today, different models exist – but all are based on the derivation from the slope gradient (Seconi and Catani 2008).

Therefore, according to DeRose (1996) and Salciarini et al. (2006), the correlation between the soil thickness z and the slope angle β (Formula 3) is given as an exponential function, where

$$z = 7.72 \times e^{-0.04^{*}\beta}. \quad (3)$$

Table 1 Soil thickness classes according to specified slope angle ranges in the case study Lauterbrunnen, Switzerland (GEOTEST AG 2011)

Slope angle [°]	Soil thickness [m]
<20°	3.0
20°–25°	2.5
25°–30°	2.0
30°–35°	1.5
35°–40°	1.0
40°–45°	0.75

The model SliDisp uses a similar approach. Here six different slope angle classes with their corresponding depth of bedrock interface are specified (Table 1). The better the knowledge about local conditions, the more precisely the soil thickness can be defined.

AGN (2004) as well as the results of different field campaigns (Liniger 2006; GEOTEST AG 2011) show that especially slopes with angles from 20° to 45° are susceptible to shallow landslides. Generally, with such steep slopes the soil thickness varies between 0.2 and 0.5 m on topographic ridges, and reaches 3.0 m in hollows (Riner 2009).

Geotechnical Parameters

Depending on the local geology and the subsoil type, the geotechnical characteristics (such as permeability, angle of internal friction, cohesion) and the spatial pattern of loose rock are specified. Geological and geotechnical maps, borehole data, and soil maps can also serve as database for this task. Additionally, field mapping and geotechnical analysis of the subsurface can be realized if necessary.

For simulation purposes, areas with the same geotechnical characteristics (subsoil classes) are merged into polygons. The mean values for permeability, angle of internal friction ϕ', and cohesion c′ are referred to all assigned polygons. The geotechnical characteristics of the subsoil are assumed to be uniform within a single polygon and homogeneously distributed (Liu and Wu 2008).

Permeability

According to Hölting and Enke (1996), the permeability of loose rock can be estimated approximately, depending on the distribution of the grain size. Six different permeability ranges are generally considered, from gravel to mid-size sand to clay (Table 2).

The classification adopted in SliDisp considers six classes (according to VSS 1999 and Wittke 1984). For each class, a permeability number from 1 to 6 is designated. Within the model, this number is translated into a coefficient (m = 0.15–0.9) and is taken as the basis for calculating the groundwater level.

Areas with different grain sizes and different permeability may constitute hydraulic barriers and are more common

Table 2 Derivation of the permeability coefficient "m" from different grain sizes (VSS 1999; Riner 2009). Example from Lauterbrunnen case study, Switzerland (GEOTEST AG 2011)

Class	Respective grain size	Permeability (k-values)	Permeability coefficient m
1	Pure gravel	$<10^{-8}$	0.15
2	Sand	10^{-7} bis 10^{-8}	0.30
3	Fine sand	10^{-6} bis 10^{-7}	0.45
4	Silty sand	10^{-4} bis 10^{-6}	0.60
5	Clayey silt	10^{-2} bis 10^{-4}	0.75
6	Clay	$>10^{-2}$	0.90

in heterogeneous soils. The probability for increasing positive pore pressures is higher at such locations (Lourenco et al. 2006). Therefore soils identified as heterogeneous are ranked one class lower (Riner 2009). For example, heterogeneous silty sand will not achieve the permeability number 3, but 2.

Angle of Internal Friction (φ′)

The characteristic value of the internal friction angle (φ′) of the subsoil was determined by shear experiments or derived from existing tables with indicated soil parameters for different underground types (VSS 1999). If no laboratory datasets from shear experiments are available the definition of the parameters follows the instructions of Liener (2000) and Riner (2009). The determination of φ′, c′ and permeability is based on the weathering product of the different geological units (bedrock). By defining the grain size distribution and potential of erosion of the weathering product of the bedrock it will be possible to determine φ′, c′ by the standard USCS classification categorized in VSS (1999). An example is given in Fig. 4 for a limestone bedrock. Its weathering product is classified according to the USCS classification as SC with the characteristic geotechnical parameters.

Cohesion (c′)

Very often the spatial distribution of the cohesion c′ is an unknown parameter. Furthermore cohesion varies depending on the natural moisture content and may disappear altogether with total saturation of the subsoil. Due to these uncertainties, several model approaches minimize the influence of cohesion (Guimarães et al. 2003) or ignore it (Rickli 2001; Rickli and Bucher 2003). The experiences made with SliDisp show that cohesion can be considered in the model (Liener 2000; Tobler and Krummenacher 2004; Riner 2009).

Root Cohesion WK

Vegetation plays an important role in the stability of slopes. Among experts, it is disputed whether the root strength should be acknowledged in the stability formula or not. Quantitative performed measurements prove that the root

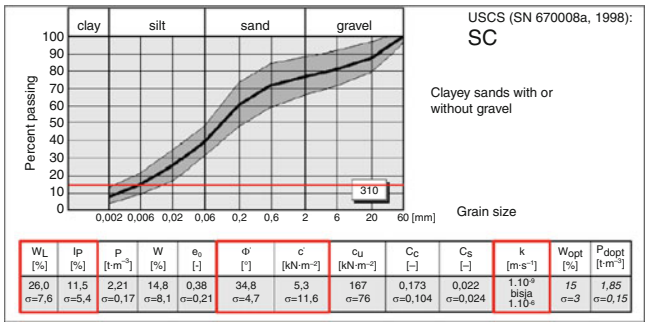

Fig. 4 Soil-parameters of clayey sands with or without gravel (*SC*) and grain-size distribution. The *red line* marks the 15 % passing line which defines the characteristic parameters wL und IP, the permeability (k-value) und shearing parameters φ′ und c′ (VSS 1999)

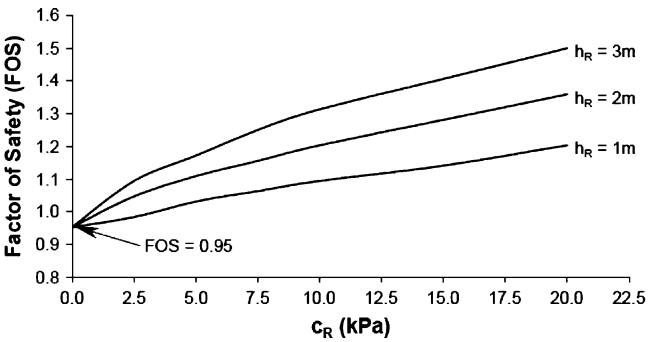

Fig. 5 Variation of factor of safety with different depths of root zones (*hR*) applying the root cohesion (*cR*) where c′ = o and vegetation extends entirely over the ground surface, including the upper slope, slope surface, and slope toe (Chok et al. 2004)

system may serve as reinforcement, and therefore may strengthen the stability of the soil (Schmidt et al. 2001). The calculation of stability acknowledged the root strength (WK) as additional cohesion force (Meisina and Scarabelli 2007). Chok et al. (2004) describe the influence of root cohesion on the factor of safety F for different depths of root zones (Fig. 5). F increases as the apparent root cohesion c_R increases. It is noted that, when the entire slope is protected by vegetation, the effects on F are significant. For example, when $h_R = 1$ F is increased by 26 % for $c_R = 20$ kPa. The increase is even more significant with a deeper root zone (higher h_R).

Hales et al. (2009) describe the spatial variability of root cohesion in landslide-prone forests. Root tensile forces were consistent among most of the tree species measured. They postulate higher mean root cohesive strength on noses (~10 kPa) than in slopes and hollows (5.5 kPa). It is obvious that the variation in root cohesion between different vegetation communities must be significant. But after Schmidt et al. (2001) the variation is quantifiable.

In the model SliDisp$^+$ the root cohesion is taken into account as a semi-empiric value between 2 and 7 kN/m^2,

depending on the relevant soil thickness and characteristics of vegetation (such as condition, age, and type of the forest (Riner 2009)). Actual investigations focus on this aspect.

Calculation of the Ground Water Level (m*z)

One of the most difficult issues in landslide susceptibility modeling is to determine the average height of totally saturated subsoil or soil. Statistical ground water models are very often used to calculate the slope stability. These models do not consider the influence of external aspects (such as precipitation, snow melt) on the temporal changes in ground water levels. As for other models, SliDisp assumes a statistical ground water level running parallel to the sliding surface.

The ground water level is the product of soil thickness z and a permeability controlled coefficient m (cf. Fig. 6, Table 2). According to Sidle and Ochiai (2006), this calculation helps to achieve an improved estimation of the stability. To consider the influence of the topographical convergence at hollows and noses the ground water level is modified by an index "t". Cox and Davies (2002) as well as Yang et al. (2005) describe the relationship between the permeability and the topographic index (TI, cf. Formula 2) by the soil-topographic index, which is a modified TI that includes a soils component (soil depth and saturated permeability data). Both indexes are part of the topmodel concept (Quinn et al. 1995). Based on Agnew et al. (2006) and Riner (2009) the semi-empiric parameter t has a range of −0.1–0.0 on noses and 0.1–0.25 in hollows (Table 3).

Thus, the ground water level implemented in the model SliDisp+ is calculated by:

$$\text{Depth of saturated zone} = (\text{m} + \text{t})^{*}\text{z} \tag{4}$$

where z = soil thickness, m = permeability coefficient, and t = empiric index for topographic influence. There is a hydrological condition for m: $0 < \text{m} \leq 1.0$. Negative values will be corrected to 0, values >1 to 1.0 (complete saturation).

Upgrade from SliDisp to SliDisp+

The process model SliDisp has been upgraded with two important new features. The approach to calculate the ground water level in the subsoil or in debris has been changed and the impact of joint water (KW) has been considered by implementing a correction value to the stability formula (Formula 5, red circles for new features). Both features are described in the following two sections.

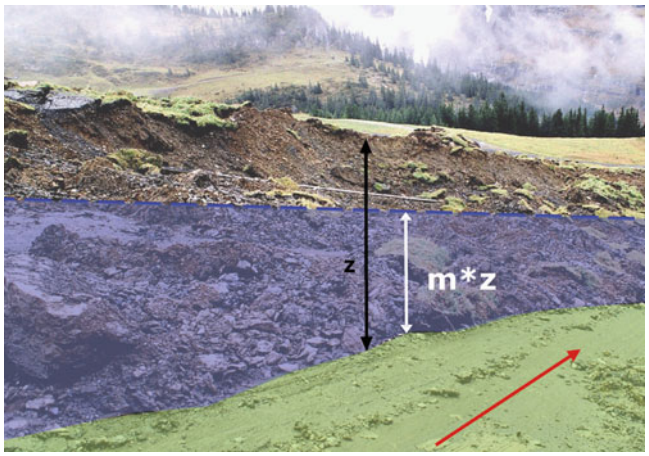

Fig. 6 Visualization of the saturated zone m*z on an open landslide scarf, with z = soil thickness and m = permeability coefficient. *Red arrow* slip surface and slip direction

Table 3 Topographic-Index classes with indication of "t" value for the case study Lauterbrunnen, Switzerland (GEOTEST AG 2011)

Class	Topo-index range	Description	Index "t" [−]
1	<3.0	Nose	−0.1
2	3.0–5.7	Slope	0
3	5.7–8.1	Hollows	0.1
4	>8.1	Channels	0.25

$$F = \frac{WK + c' + (\gamma \cdot z \cdot cos^2\beta - \gamma_w \cdot gw \cdot cos^2\beta) \cdot tan\varphi' - KW}{\gamma \cdot z \cdot sin\beta \cdot cos\beta} \tag{5}$$

Calculation of the Saturated Zone (gw) According to SliDisp+

According to the calculation of the saturated zone in SliDisp, the ground water level is proportional to the soil thickness (Lineback Gritzner et al. 2001). Therefore the proportion of saturated material (m + t)*z (Formula 4) referring to the total thickness of subsoil z remains constant. This is formally not correct. Then shallow layers may show a proportionally higher ground water level than thicker soils (Sidle and Ochiai 2006).

With SliDisp+ the ground water level (m + t)*z is adjusted by using an empirically determined height, which varies depending on the thickness of the soil. Following this calculation, the water saturated zone may be enlarged in shallow soils (thickness of 0.3–1 m) by maximally 20 cm; it may be lowered by maximally 70 cm in deep soils of 1–3 m. The corrected ground water level is implemented as a parameter called "gw" in the stability formula (Formula 5).

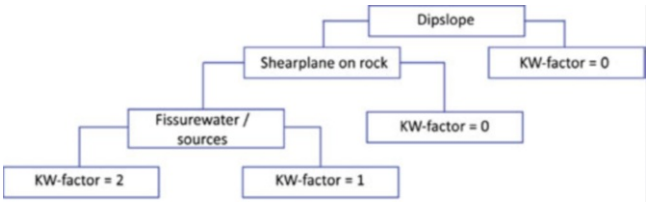

Fig. 7 Flow chart for the definition of KW-coefficient (Riner 2009)

Fissure Water Coefficient (KW)

At locations where joints and cracks crop out beneath the covering soil layer, enormous pore water pressures may develop. The joint water infiltrates into the potential slip surface and may therefore support the triggering of shallow landslides.

The model SliDisp$^+$ implements the susceptibility of joint water as a qualitative correction value KW into the stability analysis (Fig. 7). KW may have the value 0 (small influence) or 2 (large influence); it is taken into account as a "negative" cohesion in the stability formula (Formula 5).

The parameter KW has to be determined by field investigations. Therefore the orientation of the bedrock is essential. Following the decision tree in Fig. 7, the KW parameter is easy to define.

Case Study Lauterbrunnen, Switzerland

In 2010 model calculations with SliDisp$^+$/SliDepot (runout) were carried out within the settlements (approx. 30 km^2) of the community of Lauterbrunnen during a review of the existing hazard map (GEOTEST AG 2003).

Lauterbrunnen is situated in central Switzerland at an altitude of 800–1,500 m a.s.l. (Fig. 8). The bedrock consists mainly of schist and sandstones of the Aalenian and the Bajocian (Dogger), sandstones of the Oxfordian and Callovian, as well as compact Malm lime and sediments from the Tertiary (Günzler-Seiffert 1962). The rock is folded in a large scale and disrupted by several steep tectonic displacements. The weathering-resistant lime and the sandstones form striking steep rock walls falling towards the valley bottom (Fig. 9). The schists of the Aalenian are very susceptible to landslides (GEOTEST AG 2003, 2007).

On both sides of the valley the rock is covered by silty moraines, dislocated slope debris and historic deposit from rock falls. The bottom of the valley consists of fine-grained flood sedimentation from the river and shows a heterogeneous layering of material.

Fig. 8 Investigation area for the review of the hazard map in Lauterbrunnen, central Switzerland (Swissmap 2011)

Fig. 9 View from the South through the Lauterbrunnen valley with the steep cliffs of limestone and landslide-susceptible deposits in the valley bottom

Model Input

A detailed geological map is available for the investigation area (1:25,000) as well as numerous event documentations. Furthermore, field studies were made for the review of the hazard map (GEOTEST AG 2011). Eighteen different subsoil types were identified in total. They were classified according to USCS (Table 4) and the described method in previous chapters. The relevant geotechnical parameters

Table 4 Classified underground with input parameters for SliDisp+ (GEOTEST AG 2011)

Type of lose rock/soil	USCS-classification	Φ' [°]	C′	PC
Aalenian schist	CL–ML	32.7	0.4	2
Alluvion	GP	38	0	5
Marl	CL	30.7	4.2	2
Moraine	SC	34.8	5.3	2
Tertiary	ML >30 %	28.8	11.7	2
Triassic	ML	33.9	6.5	2
Slope debris	SP–SM	34.4	0	3

PC indicates permeability class number (cf. Table 2)

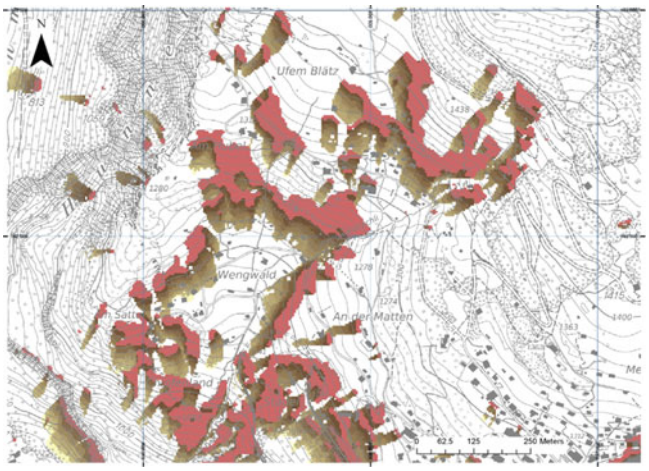

Fig. 10 Section of the calculated shallow landslide areas in Lauterbrunnen (*red* = source modeled with SliDisp+; *brown-yellow* = runout modeled with SliDepot; GEOTEST AG 2011)

(φ′, c′ and permeability DL) were derived from laboratory tests on four representing samples (Wakatsuki and Matsukura 2008).

Results

Figure 10 shows the source areas (detachment zones of shallow landslides in red) calculated with SliDisp+ as well as the runout areas (brown-yellow) calculated with SliDepot (Tobler et al. 2011; GEOTEST AG 2011). SliDepot is an absolute GIS modeling. Starting with the data from the defined source zones the distribution of material in a downhill flow direction is calculated. The model focuses on the amount of water within the shallow landslide that will be reduced during the natural process. Finally the lack of process water will determine the point where the distribution of material stops (Tobler et al. 2011).

Starting from the dark red areas in Fig. 10 (calculated source locations for shallow landslides) the runout areas are modeled by stepwise reducing the original water content

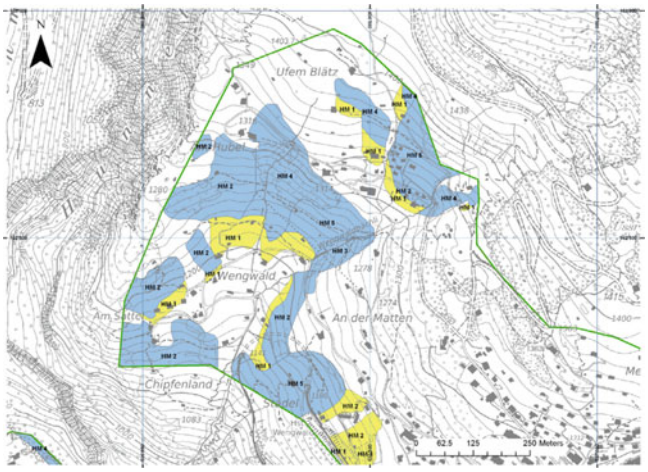

Fig. 11 Section of the actual hazard map for shallow landslide processes of Lauterbrunnen with hazard levels (*blue* and *yellow areas*; *green* = investigation area; GEOTEST AG 2011). The numbers indicate the field in the intensity-probability diagram (AGN 2004)

through max. eight discharge steps, each of 20 m. For Lauterbrunnen an excellent event register exists. So the final number of necessary discharge steps and therefore the maximal runout range has been calibrated with silent witnesses from events in 1999 and the event register (GEOTEST AG 2007). The average angle of reach of all shallow landslides is 27° and lies within the range postulated by Dai and Lee (2002).

The model results indicate the landslide-prone areas. For creating a hazard map process intensities have to be added. Therefore the additional field investigations focused (a) on the verification of modeled areas (detachment zones as well as runout) and (b) on the definition of the process intensities. AGN (2004) defines the different process intensities in hazard mapping. The actual hazard map is shown in Fig. 11. Comparing the calculated areas with the hazard map it is obvious that nearly all hazard zones have a smaller extension than the modeled process areas. The model results suit for hazard indication maps, but are not precise enough to derive directly hazard maps.

Conclusion

Many uncertainties are not considered in the calculation of the detachment zones for shallow landslides. These uncertainties underlying the model may include the type of material, mechanism of failure, ground water, the volume of failure and the geology. The parameters obtained are applicable to predict the shallow landslide susceptibility on regional scales. By employing a GIS, the analysis helps to identify conflict zones between damage potentials and process areas, which again enables efficient spatial planning or the definition of measurements to protect human lives and the infrastructure (Casadei et al. 2003).

The quality of the results correlates directly to the quality of the input parameters (e.g. knowledge of the underground, of the hydrogeological system, and of the soil cover). With the implementation of soil parameters, joint water (pressure) and a corrected, quasi-realistic ground water level, the model may soon be used directly for hazard mapping. The focus for future investigations has to be on the determination of subsurface water flows. Especially in shallow seated areas, macro pores like mouse channels may have an important influence on the stability of slopes. Observations during heavy rainfall events in the Lauterbrunnen valley lead to the assumption that slopes with high macro pore rates are better drained than others.

Acknowledgments We would like to thank Karen Bennett and Nigel Hulbert to improve the manuscript.

References

AGN (2004) Gefahreneinstufung Rutschungen i.w.S. Permanente Rutschungen, spontane Rutschungen und Hangmuren. Entwurf, Bern

Agnew JA, Lyon S, Marchant PG, Collins VB, Lembo AJ, Steenhuis TS, Walter MT (2006) Identifying hydrologically sensitive areas: bridging the gap between science and application. J Environ Manage 76:63–76

Beven KJ, Quinn P, Romanowicz R, Freer J, Fisher J, Lamb R (1995) TOPMODEL and GRIDATB, a user guide to the distribution versions (95.02). CRES Technical Report 110 (2nd edn). Lancaster University

Casadei M, Dietrich WE, Miller NL (2003) Testing a model for predicting the timing and location of shallow landslide initiation in soil-mantled landscapes. Earth Surf Process Landf 28:925–950

Chok YH, Kaggwa WS, Jaksa MB, Griffiths DV (2004) Modelling the effects of vegetation on stability of slopes. In: Proceedings of the 9th Australia New Zealand conference on geomechanics, Auckland, vol 1, pp 391–397

Cox JW, Davies PJ (2002) The duration of soil saturation: point measurements versus a catchment-scale method. In: McVicar TR, Li R, Walker Jl, Fitzpatrick RW, Chanming L (eds) Regional water and soil assessment for managing sustainable agriculture in China and Australia. ACIAR monograph 84, pp 224–230

Dahal RK (2008) Predictive modelling of rainfall-induced landslide hazard in the lesser Himalaya of Nepal based on weights-of-evidence. Geomorphology 102:496–510

Dai FC, Lee CF (2002) Landslide characteristics and slope instability modeling using GIS, Lantau Island, Hong Kong. Geomorphology 42:213–228

DeRose RC (1996) Relationships between slope morphology, regolith depth, and the incidence of shallow landslides in eastern Taranaki hill country. Z Geomorphol Suppl. Bd. 105:49–60

GEOTEST AG (2003) Technischer Bericht zur Gefahrenkarte Lauterbrunnen, Nr. 00063.5, Zollikofen (unpublished)

GEOTEST AG (2007) Lauterbrunnen, Rutschung Gryfenbach, Synthese und Prognosen, Report Nr. 94152.26, Zollikofen (unpublished)

GEOTEST AG (2011) Lauterbrunnen, Naturgefahren, Bericht zur Teilrevision Gefahrenkarte, Nr. 10151.01, Zollikofen (unpublished)

Glade T, Anderson M, Crozier MJ (2005) Landslide hazard and risk. Wiley, Chichester, 824 p

Godt JW, Baum RL, Savage WZ, Salciarini D, Schulz WH, Harp EL (2008) Transient deterministic shallow landslide modelling: requirements for susceptibility and hazard assessments in a GIS framework. Eng Geol 102(3–4):214–226

Griffiths J, Mather AE, Hart AB (2002) Landslide susceptibility in the Rio Aguas catchment, SE Spain. Q J Eng Geol Hydrogeol 35:9–18

Guimarães RF, Montgomery DR, Greenberg HM, Fernandes NF, Gomes RA (2003) Parameterization of soil properties for a model of topographic controls on shallow landsliding: application to Rio de Janeiro. Eng Geol 69:99–108

Günzler-Seiffert H (1962) Geologischer Atlas der Schweiz 1:25,000, Blatt 6 Lauterbrunnen. Schweizerische Geologische Kommission

Guzzetti F, Reichenbach P, Ardizzone F, Cardinali M, Galli M (2006) Estimating the quality of landslide susceptibility models. Geomorphology 81:166–184

Hales TC, Ford CR, Hwang T, Vose JM, Band LE (2009) Topographic and ecologic controls on root reinforcement. J Geophys Res 114: F03013. doi:10.1029/2008JF001168

Hölting B, Enke F (1996) Einführung in die Allgemeine und Angewandte Hydrogeologie, 5th edn. Stuttgart Verlag, Stuttgart

Kalos MH, Whitlock PA (1986) Monte Carlo methods, vol 1, Basics. Wiley, New York

LaCasse S, Nadim F (1996) Uncertainties in characterising soil properties. Geotechnical Special Publication No. 58, vol 1, pp 49–75

Liener S (2000) Zur Feststofflieferung in Wildbaechen. Dissertation, Geographica Bernensia, Bern

Liener S, Kienholz H, Liniger M, Krummenacher B (1996) SDLISP – a procedure to locate landslide prone areas. In: Senneneset K (ed) Landslides. Balkema, Rotterdam, pp 279–284

Lineback Gritzner M, Marcus WA, Aspinall R, Custer SG (2001) Assessing landslide potential using GIS, soil wetness modeling and topographic attributes, Payette River, Idaho. Geomorphology 37:149–165

Liniger M (2006) Die Herausforderung der Gefahrenprognose bei Massenbewegungen: Rutsch- und Sturzprozesse. Bull Angew Geol 11(2):75–88

Liu CN, Wu CC (2008) Integrating GIS and stress transfer mechanism in mapping rainfall-triggered landslide susceptibility. Eng Geol 101:60–74

Lourenco SDN, Sassa K, Fukuoka H (2006) Failure process and hydrologic response of a two layer physical model: implications for rainfall-induced landslides. Geomorphology 73:115–130

Meisina C, Scarabelli S (2007) A comparative analysis of terrain stability models for predicting shallow landslides in colluvial soils. Geomorphology 87:207–223

Paulin GL, Bursik M (2009) Assessment of landslides susceptibility – LOGISNET: a tool for multimethod, multilayer slope stability analysis. VDM Verlag Dr. Müller, Saarbrucken

Quinn PF, Beven KJ, Lamb R (1995) The ln(a/tanb) index: how to calculate it and how to use it within the topmodel framework. Hydrol Process 9:161–182

Rickli Ch (2001) Vegetationswirkungen und Rutschungen. Untersuchung zum Einfluss der Vegetation auf oberflächennahe Rutschprozesse anhand der Unwetterereignisse Sachseln am 15.8.1997. Eidg. Forschungsanstalt (WSL), Birmensdorf, 97p

Rickli C, Bucher H, (2003) Oberflächennahe Rutschungen, ausgelöst durch die Unwetter vom 15.–16.7.2002 im Napfgebiet und vom 31.8–1.9.2002 im Gebiet Appenzell. Eidg. Forschungsanstalt (WSL) und Bundesamt für Wasser und Geologie (BWG), 75p

Riner R, (2009) Geotechnische Analysen von Lockergesteinen zur Modellierung von Rutschdispositionen im Untersuchungsgebiet Niesen. Masterarbeit Philosophisch-Naturwissenschaftliche Fakultät Universität Bern, 103 p (unpublished)

Salciarini D, Godt JW, Savage WZ, Conversini R, Baum RL, Michael JA (2006) Modeling regional initiation of rainfall-induced shallow landslides in the eastern Umbria Region of central Italy. Landslides 3:181–194

Schmidt KM, Roering JJ, Stock JD, Dietrich WE, Montgomery DR, Schaub T (2001) The variability of root cohesion as an influence on shallow landslide susceptibility in the Oregon Coast Range. Can Geotech J 38:995–1024

Seconi S, Catani F (2008) Modeling soil thickness to enhance slope stability analysis at catchment scale. In: Abstract 33rd international geological congress, Oslo. http://www.cprm.gov.br/33IGC/1345585.html

Selby MH (1993) Hillslope materials and processes. Oxford University Press, Oxford

Sidle RC, Ochiai H (2006) Landslides: processes, prediction, and land use. Water resource monograph 18. American Geophysical Union, Washington, DC

Swissmap (2011) Topographic map Lauterbrunnen, Blatt 1228. www.swisstopo.ch

Tobler D, Krummenacher B (2004) Modellierung von Anrissgebieten für flachgründige Rutschungen und Hangmuren. In: Proceedings of the 2nd Swiss geoscience meeting, Lausanne

Tobler D, Riner R, Pfeifer R (2011) Runout modeling of shallow landslides over large areas with SliDepot. In: Proceedings of the second world landslide forum, Rome

VSS (1999) SN 670 010b. Bodenkennziffern, Zürich

Wakatsuki T, Matsukura Y (2008) Lithological effects in soil formation and soil slips on weathering-limited slopes underlain by granitic bedrocks in Japan, Catena. Trans Jpn Geomorphol Union 72:153–168

Wittke W (1984) Felsmechanik – Grundlagen für wirtschaftliches Bauen im Fels. Springer, Berlin/Heidelberg, 1050 p

Yang X, Chapman GA, Young MA, Gray JM (2005) Using compound topographic index to delineate soil landscape facets from digital elevation models for comprehensive coastal assessment. In: "MODSIM" conference, Melbourne, 12–15 Dec 2005

Zolfaghari A, Heath AC (2008) A GIS application for assessing landslide hazard over a large area. Comput Geotech 35:278–285